Analysis of an Optofluidic Biochemical Sensor

Edward P. Furlani[1], R. Biswas[2], A. N. Cartwright[2] and N. M. Litchinitser[2]

The Institute for Lasers, Photonics and Biophotonics, University at Buffalo SUNY
432 Natural Sciences Complex, Buffalo, NY, **efurlani@buffalo.edu**

[2]Department of Electrical Engineering, University at Buffalo SUNY
332 Bonner Hall, Buffalo, NY

ABSTRACT

We introduce a novel optofuidic biochemical sensor in which detection is based on the contrast between the refractive index of a target biomaterial and ambient carrier fluid. The sensor consists of parallel vertical micochannels embedded in a planar substrate. The central microchannel is illuminated by a focused beam of light and the periodic spacing of the channels combined with the contrast in refractive index between the fluid and the substrate act to confine and guide the incident light down through the central channel. Sensing is achieved via accumulation of a nanoscale layer of target biomaterial on the surfaces of the the microchannels. This layer causes a shift in the optical transmission spectrum of light passing through the substrate. We demonstrate the viability of the sensor using full-wave electromagnetic analysis and study its transmission spectrum at optical wavelengths as a function of layer thickness and refractive index.

Keywords: optofluidics, optofluidic biosensor, optofluidic chemical sensor, microstructured optical waveguide sensor, planar Bragg waveguide, ARROW-based sensor.

1 INTRODUCTION

The interest in compact, portable and inexpensive biosensors for point-of-service clinical diagnostic applications has grown dramatically in recent years due in part to advances in microfluidics, especially lab-on-a-chip technology. A relatively new and promising approach to biosensing involves optofluidics where optic and fluidic functionality are integrated into a microsystem to leverage their combined advantages [1,2]. Microfluidic functionality enables compact and rapid processing of small biofluid samples, and optical functionality enables high detection sensitivity of target biomaterials within these samples. To date, various optofluidic sensing devices have been developed. Many of these utilize a detection scheme based on some form of resonant optical behavior with input/output signals carried by optical fibers or integrated waveguides. Examples of these include waveguide coupled photonic crystal resonators and Whispering Gallery Mode (WGM)-based sensors [3-7]. Such sensors are capable of high detection sensitivity, but they have potential

drawbacks both in terms of input/output coupling efficiency and ease of multiplexing, i.e. addressing multiple independent sensing stations on a single platform.
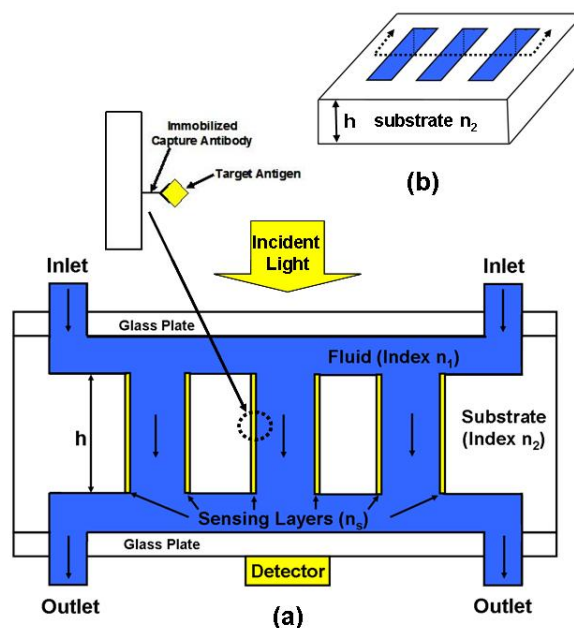

Figure 1: Optofluidic sensor: (a) cross-section showing functionalized microchannels, (b) perspective view of the sensor substrate.

In this presentation we introduce a novel optofluidic biosensor that operates in a transmission mode and can function using free-space illumination, without the need for fiber or waveguide coupled input/output signals. The sensor consists of parallel microchannels embedded in a substrate with an orientation perpendicular to its surface as shown in Fig. 1. The central microchannel is illuminated with a focused beam of light. The periodic spacing of the channels and contrast in refractive index between the carrier fluid and the substrate act to confine and guide the incident light similar to that of an antiresonant reflecting optical waveguide (ARROW) [8-11]. The transmission spectrum of the sensor is obtained using a detector positioned beneath the central microchannel. The transmission signal collected

in the detector depends on the wavelength of the light, the dimensions, periodicity and refractive index of the substrate and the refractive index of the carrier fluid. Sensing is achieved via accumulation of a thin (nanoscale) layer of target biomaterial on the surface of the microchannel walls, which are functionalized to bind with the material as it flows through the system. Detection is based on a shift in the transmission spectrum caused by the contrast in refractive index between the carrier fluid and the target biomaterial. We use 2D full-wave time-harmonic electromagnetic analysis to study the transmission spectrum of the sensor at optical wavelengths as a function of material and device parameters. Our analysis demonstrates that a detectable shift in the transmission spectrum can be achieved with nanoscale layers of biomaterial and with little contrast in refractive index between the biomaterial and carrier fluid. As such, the sensor holds potential for compact and low-cost biosensing applications.

2 MODELING AND RESULTS

We study the spectral response of the biosensor using 2D full-wave time-harmonic field analysis. The COMSOL RF solver, which is based on finite element analysis (FEA), is used for the analysis. We apply perfectly matched layers (PMLs) at the top and bottom of the computational domain to reduce backscatter from these boundaries (Fig. 2). Similarly, we impose scattering boundary conditions at the boundaries transverse to the direction of propagation to reduce backscatter from these boundaries as well. We illuminate the central microchannel with a downward directed Gaussian-like beam as shown. The incident field is generated by a time-harmonic surface current positioned immediately below the upper PML. The current flows in and out of the page as indicated.

For our initial analysis we choose the central microchannel to have a width of 4 μm. The adjacent side channels are 4 μm wide and spaced 4 μm apart, center-to-center. The fluidic feed channels above and below the substrate are 12 μm in height. The upper and lower PML layers are immediately above and below the upper and lower fluidic feed channels, respectively. The fluid and substrate have a refractive index of $n_1 = 1.33$ (H2O) and $n_2 = 1.45$ (SiO2), respectively. We compute the time-averaged power at the top and bottom of the central microchannel at optical wavelengths. We take the ratio of these values to determine the transmission through the channel,

$$T(h, \lambda, w_s, n_s) = \frac{P_{out}(h, \lambda, w_s, n_s)}{P_{in}(h, \lambda, w_s, n_s)} \quad (1)$$

The transmission depends on several variables including the height h of the microchannels (Fig. 2), the wavelength λ of the incident light and the width w_s and refractive index n_s of the biolayer, among others.

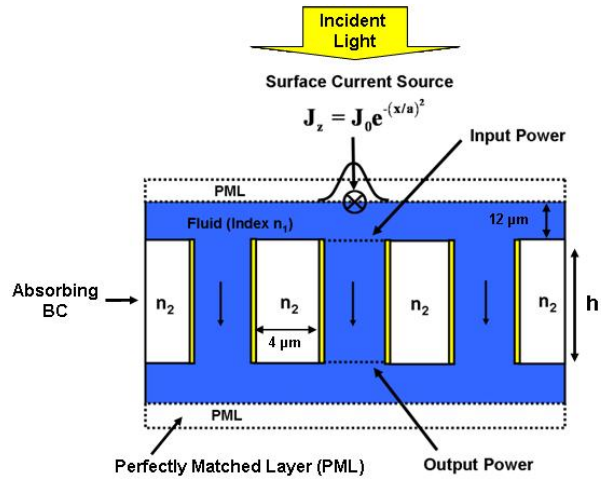
Figure 2: Biosensor computational model.

We first compute the transmission spectrum as a function of the channel height h. We impose a time-harmonic surface current below the upper PML with a Gaussian-like profile (A/m) where = 2 μm. We compute the spectral response (λ = 550-850 nm) for four different channel heights h = 30, 45, 60 and 75 μm as shown in Fig. 3. Note that the transmission spectrum exhibits more clearly defined and pronounced maxima and minima as h increases. This is desirable for sensing as detection is based on a shift in the spectrum. However, there is a practical
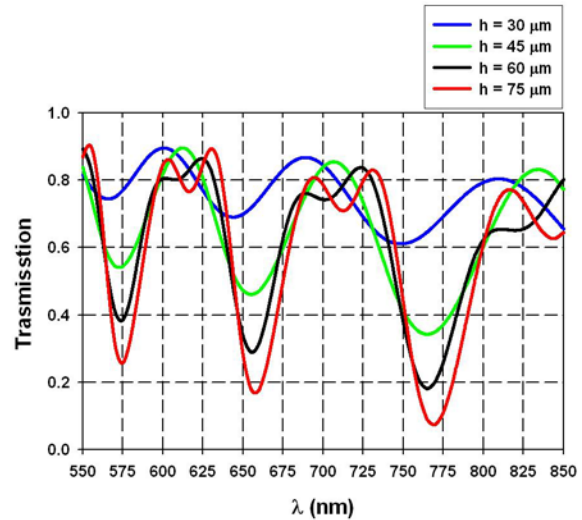

Figure 3: Transmission spectrum vs. substrate height h.

limit to the depth of the microchannel relative to its width, i.e. the aspect ratio is limited by microfabrication processes and the substrate material properties. For the remaining analysis we use an aspect ratio of 15:1, and thus for 4 μm channels we choose h = 60 μm. While this ratio might be challenging to obtain using our assumed SiO2 substrate, it

can be achieved using alternate low-loss materials such as SU8 (n_2 = 1.6-1.8).

The spectral response of the sensor can be understood by recognizing that its optical configuration is similar to a 1D photonic bandgap structure [8-11]. Light launched down the low-index central microchannel (core) will be partially guided via Bragg reflections from the periodic lateral high- and low-index layers formed by the substrate and carrier fluid, respectively. As such, the transmission minima can be estimated using a simple analytical expression that is derived using an ARROW model. The minima for a 1D ARROW structure occur at [8]

$$\lambda_m = \frac{2n_1 d}{m}\left[\left(\frac{n_2}{n_1}\right)^2 - 1\right]^{\frac{1}{2}} \quad (m = 1, 2, \ldots) \quad (2)$$

where n_1 is the index of the low-index (carrier fluid) layer and d and n_2 are the width and index of the high-index (substrate) layer. Note that the transmission spectra shown in Fig. 3 correlate well with the analytical ARROW model as the height h of the substrate increases. Specifically, as h increases the transmission spectrum converges to a plot that has three transmission minima, which correspond to m = 6, 7 and 8 in Eq. (2). The numerical analysis converges to minima at λ_6 = 770 nm, λ_7 = 660 nm and λ_8 = 578 nm, which follow from Eq. (2).

Next, we perform a parametric analysis to determine the spectral response of the sensor as a function of the refractive index of the sensing layer n_s = 1.33, 1.35,…, 1.45, (i.e. $n_1 \leq n_s \leq n_2$), which is taken to be 100 nm thick. We fix the substrate thickness h = 60 μm, and compute the transmission spectra for a range of wavelengths λ = 550-850 nm as shown in Fig. 4a. Note that the transmission minima shift toward longer wavelengths as the index of the sensing layer n_s increases. The transmission spectra exhibit a nearly linear shift of Δλ = 7 nm towards longer wavelengths for every change in refractive index of Δn = n_s – n_1 = 0.02 between the sensing layer and carrier fluid (Fig. 4b). This can be understood from the ARROW model, Eq. (2). Specifically, the sensing layer has the effect of increasing the width d of the high-index substrate layer. Let w_s denote the width of the sensing layer (set to 100 nm in the above analysis). As n_s increases towards that of the high-index substrate layer n_2, it has the effect of increasing the width of this layer $d \rightarrow d + 2w_s$. Thus, from Eq. (2) the transmission minima shift by an amount $\Delta\lambda_m$ given by

$$\Delta\lambda_m = \frac{4n_1 w_s}{m}\left[\left(\frac{n_2}{n_1}\right)^2 - 1\right]^{\frac{1}{2}} \quad (m = 1, 2, \ldots) \quad (3)$$

This formula enables an estimate of the sensitivity of the sensor and it has been verified for the present structure using our numerical models. Moreover, the thickness and index of the sensing layer can be tuned by labeling the target biomaterial with a dielectric nanoparticle of a given diameter and refractive index.
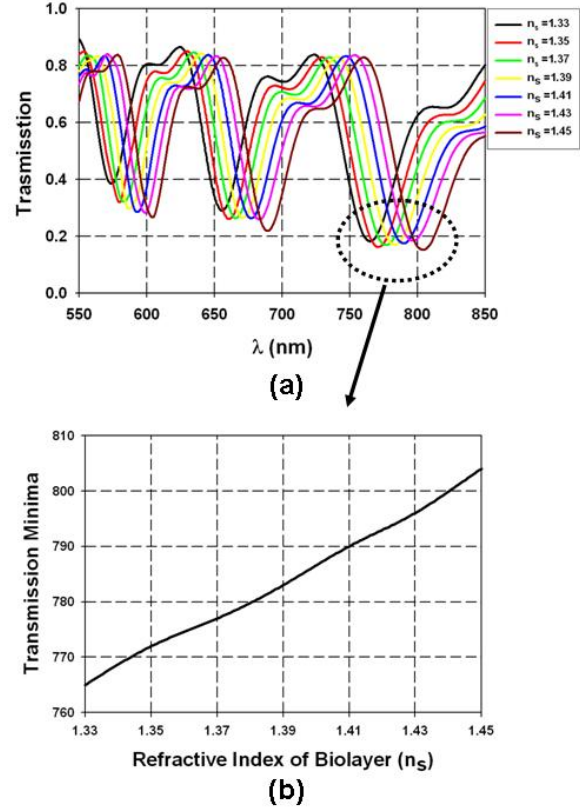

Figure 4: Transmission spectrum vs. sensing layer: (a) transmission vs. λ (parametrically vs. sensing layer refractive index n_s), (b) transmission minimum shift vs. n_s.

The preliminary analysis presented here indicates that detectable shifts in transmission can be achieved with relatively thin (nanoscale) layers of biomaterial and little contrast in refractive index between the biomaterial and carrier fluid.

4 CONCLUSIONS

The field of optofluidics is its infancy and growing rapidly, especially for applications involving biosensing. In this presentation, we have introduced a novel optofluidic transmission mode biosensor and we have studied its performance using 2D full-wave time-harmonic field analysis. The sensor can function using free-space illumination without the need for fiber or waveguide coupled input/output signals. Our results indicate that a detectable shift in transmission can be achieved with nanoscale layers of biomaterial and low contrast between the biomaterial and carrier fluid. As such, the biosensor holds potential for compact and low-cost biosensing applications.

REFERENCES

[1] C. Monat, P. Domachuk and B. J. Eggleton Integrated optofluidics: A new river of light Nature Photonics 1 2, 106-114 (2007).

[2] D. Psaltis, S. R. Quake and C. H. Yang, Developing optofluidic technology through the fusion of microfluidics and optics, Nature 442 7101, 381-386 (2006).

[3] H. Schmidt and A. R. Hawkins, Optofluidic waveguides: I. Concepts and implementations Microfluidics and Nanofluidics, 4 1-2, 3-16 (2008).

[4] F. Vollmer, D. Braun, A. Libchaber, M. Khoshsima, I. Teraoka, and S. Arnold, Protein detection by optical shift of a resonant microcavity, App. Phys. Lett. 80 4057-4059 (2002).

[5] A. Yalcin, K.C. Popat, J.C. Aldridge, T.A. Desai, J. Hryniewicz, N. Chbouki, B.E. Little, O. King, V. Van, S. Chu, D. Gill, M. Anthes Washburn, and M.S. Unlu, Optical sensing of biomolecules using microring resonators. IEEE J. Sel. Topics in Quantum Electronics, 12(1): p. 148 155 (2006)

[6] A. M. Armani, et. al, Label Free, Single Molecule Detection with Optical Microcavities, Science 317 783 (2007)

[7] M. R. Lee, P. Fauchet, Two-dimensional silicon photonic crystal based biosensing platform for protein detection, Opt. Express 15, 4530-4535 (2007)1. C. Monat, P. Domachuk and B. J. Eggleton, Nature Photonics, 1, 106-114 (2007).

[8] J. A. M. Zheltikov, Ray-optic analysis of the (bio)sensing ability of ring-cladding hollow waveguides, Appl. Opt. 47, 3 474-479 (2008).

[9] N. M. Litchinitser, A. K. Abeeluck, C. Headley, and B. J. Eggleton, Antiresonant reflecting photonic crystal optical waveguides, Opt. Lett. 27, 1592 (2002).

[10] N. Litchinitser, S. Dunn, P. Steinvurzel, B. Eggleton, T. White, R. McPhedran, and C. de Sterke, Application of an ARROW model for designing tunable photonic devices, Opt. Express 12, 1540 (2004).

[11] N. M. Litchinitser and E. Poliakov, Antiresonant guiding microstructured optical fibers for sensing applications, Appl. Phys. B 81, 347-351 (2005).